PERGAMON

Deep-Sea Research II 50 (2003) 119–139

DEEP-SEA RESEARCH
PART II

www.elsevier.com/locate/dsr2

A comparison of in-situ float velocities with altimeter derived geostrophic velocities

Olaf Boebel[a,b,c,*], Charlie Barron[d]

[a] *Alfred Wegener Institute for Polar and Marine Research, P.O. 120161, 27515 Bremerhaven, Germany*
[b] *Graduate School of Oceanography, University of Rhode Island, Narragansett, RI 02882, USA*
[c] *Department of Oceanography, University of Cape Town, 7701 Rondebosch, South Africa*
[d] *Naval Research Laboratory, Stennis Space Center, MS 39519, USA*

Abstract

Satellite borne altimetric data are of increasing prominence for assimilation in ocean circulation models and interpretation of localized in-situ measurements. Physically, geo-referenced sea-surface height (SSH) data products are mostly referenced relative to a long-term SSH mean, and consequently called SSH-anomalies. The Modular Ocean Data Assimilation System (MODAS) adds climatological SSH fields to provide space–time interpolated absolute steric SSH fields. This, in theory, should provide realistic geostrophic surface velocities and flow patterns, including quasi-permanent features such as western boundary currents or free jets. This study compares such data for the wider Agulhas Retroflection region with co-located, simultaneous velocity measurements from Cape of Good Hope Experiments (KAPEX). KAPEX used ship-borne Acoustic Doppler Current Profiles (ADCP) and neutrally buoyant RAFOS (Ranging and Fixing of Sound) floats at intermediate depths to obtain in-situ velocity data.

Correlation coefficients of MODAS-2D geostrophic and RAFOS subsurface flow directions fall between 0.8 and 0.9 with a typical error less than 0.05. The high correlation suggests that MODAS-2D provides a correct depiction of anticyclonic/cyclonic flow patterns in this region, making it a useful tool to describe the Agulhas Retroflection. Root-mean-square differences between velocities as measured by the various data sources rage between 20 and 30 cm s^{-1}, lying between the natural variability observed for the intermediate and surface layers. Decreasing *slope* parameters of linear regressions between MODAS, RAFOS and ADCP velocities reflect the baroclinic velocity shear. Slope equals 1 at surface and decreases to 0.4 at depths below 1000 m. Offsets of linear regression of these fits are not significantly different from zero, except for the zonal component in the Agulhas Return Current (5–10 cm s^{-1}). This discrepancy suggests a missing meridional gradient in this region's climatological signal that is added to the SSH anomaly field within MODAS.

1. Introduction

Altimetric data from the TOPEX/POSEIDON (Fu et al., 1994; Cheney, 1995) and ERS (ESA, 2001) satellite missions are arguably the most important information currently used to constrain basin-scale assimilating ocean circulation models.

*Corresponding author. Alfred Wegener Institute for Polar and Marine Research, P.O. 120161, 27515 Bremerhaven, Germany. Tel.: +49-471-4831-1879; fax: +49-471-4831-1797.
E-mail address: oboebel@awi-bremerhaven.de (O. Boebel).

0967-0645/02/$ - see front matter
PII: S0967-0645(02)00381-8

Offering broad coverage in space and time, these data are also increasingly utilized to interpret localized in-situ measurements, such as Eulerian or Lagrangian current meters or hydrographic sections. Numerous groups excel in an operational conversion of the altimeter range data to physically, geo-referenced sea-surface height (SSH) products. Most of these SSH products are referenced relative to a long-term SSH mean, and consequently called SSH-*anomalies*.

In Contrast, the US Naval Research Laboratory (NRL) at Stennis Space Center, Mississippi, USA provides operational global *absolute* steric SSH fields as part of the Modular Ocean Data Assimilation System (MODAS) (Fox et al., 2002). The fields, called MODAS-2D SSH or simply SSH hereinafter, are largely representative of the movement of water, and are based on a merger of TOPEX/POSEIDON, ERS-2 and climatological hydrographic data.[1] Joining TOPEX/POSEIDON with ERS-2 has been shown to better capture the mesoscale signal (Koblinsky et al., 1992; Blayo et al., 1997; Le Traon and Dibarboure, 1999; Ducet et al., 2000). The addition of a climatological mean surface elevation field leads to an improved representation of stable oceanographic features, such as quasi-permanent currents, which otherwise would be masked in the anomaly field.

This improvement is of particular relevance for our region of interest, the oceans around southern Africa and the embedded Agulhas Retroflection. Here a transition occurs between a regime dominated by the mean flow (the persistent Agulhas and the Agulhas Return Currents) and a region dominated by the eddy field, i.e. the adjacent Cape Basin. Fig. 1 exemplifies the difference between SSH-anomaly and the corresponding absolute MODAS-2D SSH fields. While the Agulhas Current (which flows along the East African shelf) and Agulhas Return Current are missing from the top panel (SSH-anomaly), they are clearly visible in the bottom panel (absolute SSH).

To what degree does MODAS-2D SSH provide an adequate representation of the upper ocean circulation? Obviously, this question has to be addressed region by region, as its answer depends on the underlying mean circulation field entering the calculation. A direct validation of MODAS-2D SSH could be achieved by comparison with tidal gauges, such as Global Positioning System (GPS) tracked buoy heights (Key, 1997), but no such data are available to us. Alternatively, geostrophic surface velocities derived from MODAS-2D SSH can be compared against in-situ velocity measurements, an approach that suits us well, due to a large number of neutrally buoyant RAFOS (Ranging and Fixing of Sound) float trajectories available for this region from the Cape of Good Hope Experiments (KAPEX).

Comparisons between in-situ and satellite altimeter derived geostrophic currents have been performed previously, but for other regions, SSH products, and in-situ instruments. For the western tropical Pacific, Yu et al. (1995) compared satellite-tracked drogued surface drifters with monthly maps of absolute SSH based on a seasonal Levitus climatology (1982) and SSH-anomalies. Using 91 data points, the Yu et al. (1995) comparison of co-located drifter and altimetric velocities indicated a statistically significant correlation (at the 95% level) between velocity components from the two data sets with $r = 0.92$ (zonal) and 0.76 (meridional).

In the California Current, Kelly et al. (1998) compared low-passed velocities from surface drifter and moored Acoustic Doppler Current Profiler (ADCP) data with geostrophic velocities from an absolute SSH product based on a combination of SSH anomalies, mean drifter velocities, and hydrographic data. The comparison between approximately 600 collocated geostrophic and drifter velocities orthogonal to the altimeter sub-track results in a significant correlation coefficient of 0.73. Kelly et al. (1998) then succeeded to show that remaining uncorrelated drifter velocity component is correlated with wind-driven Ekman transport. The later result is further

[1] While NRL uses MODAS-2D SSH fields as input to the full MODAS system or for assimilation into their NRL Layered Ocean Model (NLOM) to generate three-dimensional hydrographic fields of the upper 1000 m, our study focuses on the validity of the altimetric, two-dimensionally interpolated MODAS-2D SSH data only, which should be distinguished from the general MODAS or the NLOM products.

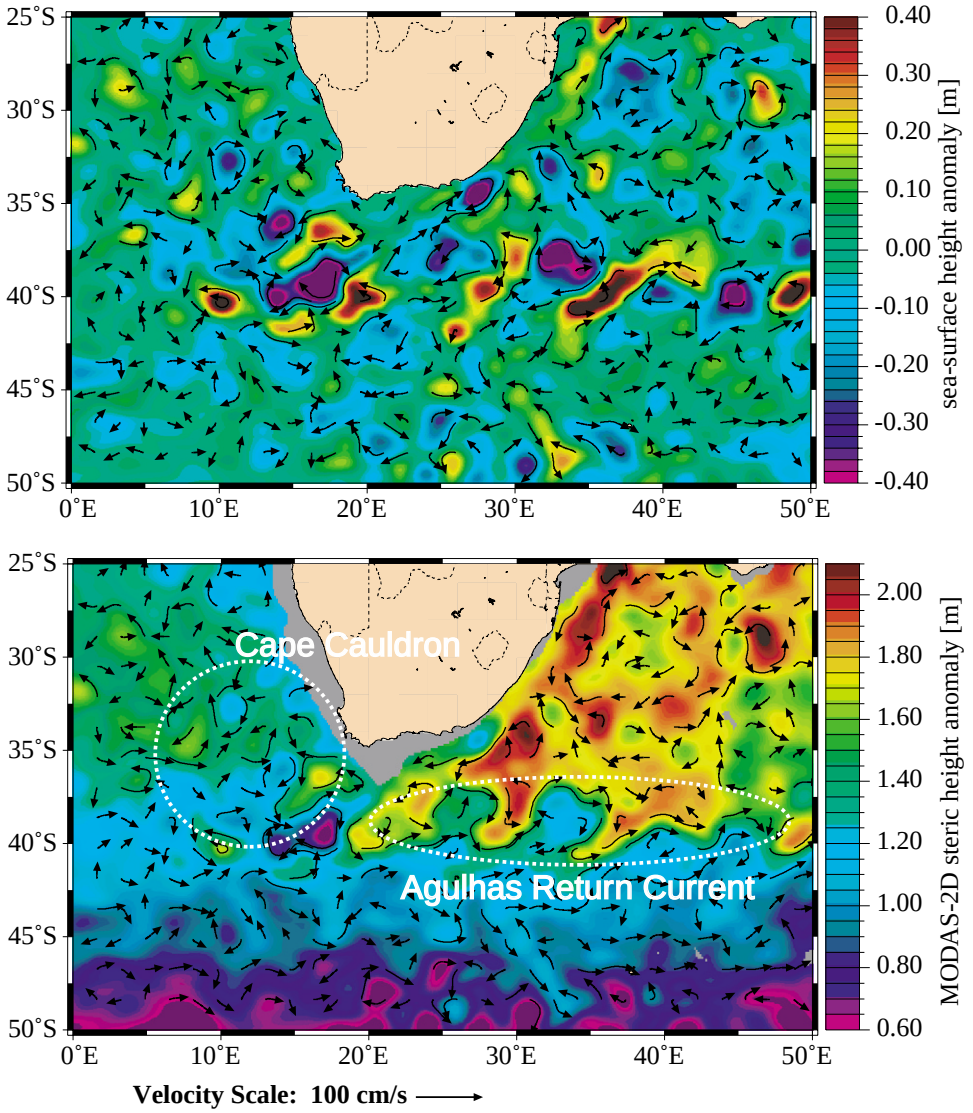

Fig. 1. SSH and derived geostrophic surface velocity in the Agulhas Return Current Region for July 1, 1998: (top) sea-surface height anomaly only, (bottom) with MODAS-2D climatology added. The continent is ochre, areas shallower than the 1000 m reference layer used in the MODAS-2D calculation are gray in the bottom panel.

supported by their comparison of mean ADCP and geostrophic SSH velocities.

The same region was evaluated in a preceding comparison of altimeter derived geostrophic velocities with velocities from moored vector averaging current meters and ADCP (Strub et al., 1997). Their comparison of the latter's cross-track velocity component with those from altimetry yields correlation coefficients between 0.59 and 0.73. The comparison results in total root-mean-square (rms) differences of 7–8 cm s^{-1} between altimeter geostrophic velocities and in-situ velocities below the Ekman layer. They (Strub et al., 1997) find this value comparable to the spatial rms difference between neighboring moorings due to small-scale variability.

Zlotnicki et al. (1993) studied the feasibility of measuring the weak surface current of the Cape Verde Frontal Zone with altimetry by comparing, amongst other methods, shallow current meter velocities and geostrophic velocities from Geosat altimetric sea level. Obtaining correlation coefficients between 0.32 and 0.90 they noted a geographical dependency of the correlation quality. Nevertheless, they concluded that in principle weak geostrophic currents averaged over 30 days and 142 km can be measured in this region with rms errors not exceeding 2–3 cm s^{-1} (Zlotnicki et al., 1993).

The equatorial Pacific region of higher intrinsic rms velocities (25–40 cm s^{-1}) was studied by Picaut et al. (1990) by comparison of Geosat derived velocities with current meter data shallower than 50 m. They obtained velocity correlation coefficients between 0.5 and 0.8, with some outliers at the low end. The rms velocity difference varied between 15 and 30 cm s^{-1}. Most recently, a drifter/altimeter comparison by Lagerloef et al. (1999) for the same region obtained meridional dependent correlation coefficients between 0 and nearly 0.9 with rms errors of 20–30 cm s^{-1}. Joyce et al. (1990) compared Geosat altimetric and ADCP data from the Gulf Stream. When including a generic Gulf Stream SSH profile in their absolute SSH estimate, they obtained correlation coefficients between 0.76 and 0.93, while observing a rms difference of 23 cm s^{-1} for a single realization.

Summarizing the above and other studies, Ducet et al. (2000) state that correlation coefficients of altimetric/in-situ velocity components predominantly fall between 0.5 and 0.9. Their own work (Ducet et al., 2000) pivots around a statistical comparison of rms-altimeter-velocities with rms-velocities from current meters and surface drifters located nearly exclusively in the North Atlantic. The derived correlation coefficients provide hence little direct information on the agreement of the *absolute velocity fields* but primarily on the energy levels, as do comparative studies by Wunsch (1997) and Stammer and Wunsch (1999).

The above studies fall into two categories. One type focuses on the comparison of cross-track geostrophic velocities with co-located and simultaneous in-situ measurements or of the full velocity vector if the instruments had been located near cross-over points of the satellite ground tracks. The other type of study compares space-time averages of velocities and energy levels from the various data sources. In contrast to these studies, our study compares the geostrophic and in-situ 2-D velocity vectors at random data locations within a large space–time domain. "Random", in lack of any better word, describes the fact that the data locations are dictated by the daily float positions along their trajectories, or by the cruise tracks, which both have not been aligned relative to the TOPEX/POSEIDON or ERS ground tracks (Fig. 2). In contrast to the studies mentioned, the comparison made herein is by and large based on geostrophic velocities from altimetric data that were obtained by interpolation only, i.e. at locations between the space–time gaps of successive satellite passes and ground tracks.

To aid the interpretation of individual float trajectories, we are mainly interested in the proper location of the dominant quasi-stable currents and an adequate representation and propagation of mesoscale eddies as captured in the MODAS-2D SSH signal. It is less the individual geostrophic velocity estimate that is important to us, but the overall placement of the cyclonic/anticyclonic features. A first visual comparison between the propagation of mesoscale SSH features and RAFOS float trajectories suggests a striking qualitative agreement. The data are visualized in an animation of the MODAS-2D geostrophic velocity field (blue arrows) with float trajectories superposed.[2] Exemplifying the situation, a single frame of this movie is shown in Fig. 3. The floats, represented by 5-day-long red trajectory segments with heads first, drifted at intermediate depth and collected data between 1997 and 1999 as part of KAPEX (Boebel et al., 1998). Additional data (not

[2]The animation can be obtained from the corresponding author or downloaded from Elsevier's DSR-II web portal at http://www.elsevier.com/locate/dsr2. Please follow the links to this issue's table of content where electronic annexes are linked. The movie is provided as zip archive (MODAS_RAFOS_comparison.avi.zip) of 52 Mbyte size with 1430 × 1073 pixels.

shown) stem from in-situ velocity measurements made by ship-born ADCP.

Our statistical study distinguishes between instruments that floated in the vicinity of the Agulhas Return Current (ARC) and those in the south-eastern section of the Cape Basin. The selected regions (Fig. 1) represent two different oceanic regimes. One is characterized by a quasi-stable zonal current, i.e. the Agulhas Return Current (Boebel et al., 2003b), while the other region, the Cape Cauldron, is dominated by strong mesoscale variability (Boebel et al., 2003a).

2. Data

2.1. MODAS-2D velocity data

Descriptions of most aspects of MODAS-2D are given by Fox et al. (2002) and Jacobs et al. (2001). For the reader's convenience we here summarize the approach used to produce the MODAS-2D real time steric height anomaly[3] as defined in Gill (1982) or Olbers et al. (1992):

$$h = \int_0^H \frac{[v(T,S,p) - v(0^\circ, 35, p)]}{v(0^\circ, 35, p)} \mathrm{d}z, \tag{1}$$

where v is the specific volume of sea water and H is the column depth, which is set to 1000 m here. Daily MODAS-2D SSH estimates start with an optimal interpolation of the altimetric data sets onto a $1/8^\circ$ latitude $\times$ $1/8^\circ$ longitude grid to develop a field of height deviation from the altimetric mean (Eq. (2, term a)). The space–time interpolation process involved is not trivial. As illustrated by Fig. 2, large spatial gaps exist in between altimetric measurements for a given day. The spatial gaps are wide enough to easily let mesoscale feature fall "in between". MODAS-2D, using mesoscale-tuned estimates of the error covariance and propagation, adjusts the objective interpolation process to the regionally dependent observed space and time scales of ocean variability to minimize the errors caused by the undersampling (Jacobs et al., 2001; Fox et al., 2002).

The MODAS-2D steric height anomaly is approximated by adding this deviation field (Eq. (2a)) to two others: the steric height anomaly calculated from the MODAS-2D climatological mean (Eq. (2b)), and the correction for the difference between the altimetric and climatological means (Eq. (2c)).

$$\begin{aligned}
&\text{MODAS-2D real time steric height anomaly relative to 1000 m} \\
&\quad = \{\text{altimeter deviation}\} \\
&\qquad + \{\langle \text{in situ steric height anomaly rel. to 1000 m} \rangle_{\text{clim}}\} \\
&\qquad + \{\text{correction for difference in means}\}, \qquad (2)
\end{aligned}$$

$$\begin{aligned}
&= \{\text{altimeter measurement} \\
&\quad - \langle \text{altimeter measurement} \rangle_{\text{ap}}\} \qquad (2a)
\end{aligned}$$

$$+ \langle \text{in situ steric height anomaly rel. to 1000 m} \rangle_{\text{clim}} \qquad (2b)$$

$$\begin{aligned}
&+ \langle \text{in situ steric height anomaly rel. to 1000 m} \\
&\quad - \langle \{\text{in situ steric height anomaly rel. to 1000 m} \rangle_{\text{clim}}\} \\
&\quad - \{\text{altimeter measurement} \\
&\quad - \langle \text{altimeter measurement} \rangle_{\text{ap}}\} \rangle_{\text{ap}} \qquad (2c)
\end{aligned}$$

The climatological steric height anomaly is computed by integrating from the climatological pressure at 1000 m to the surface. Since the data received in the MODAS-2D processing is the altimeter deviation (Eq. (2a)), which subtracts the altimeter period mean sea-surface height, the $\langle$steric height anomaly rel. to 1000 m$\rangle_{\text{ap}}$ must be added to obtain the real time steric height anomaly relative to 1000 m. In MODAS-2D, the $\langle$steric height anomaly rel. to 1000 m$\rangle_{\text{ap}}$ term is approximated by (2b) and (2c). Correction for the difference in means was used but not described by Fox et al. (2002) (see their Appendix d for a direct comparison).

The symbol "$\langle\,\rangle_{\text{clim}}$" refers to an averaging over almost a century of hydrographic measurements used in the MODAS climatology, while

[3] Note the ambivalence of "anomaly" as used in the terms "SSH anomaly" and "MODAS-2D real time steric height anomaly". In "SSH anomaly", anomaly refers to the deviation from the altimetric mean SSH signal (averaged over the altimeter period). In "MODAS-2D real time steric height anomaly", anomaly refers to the difference between a real and an ideal water column as given in Eq. (1).

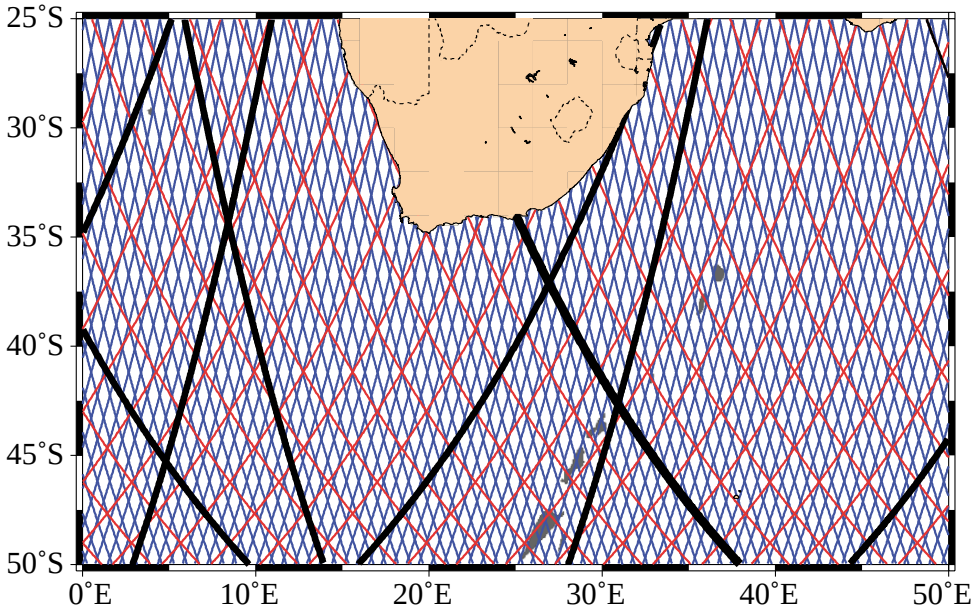

Fig. 2. TOPEX/POSEIDON (red) and ERS (blue) ground tracks around southern Africa. Black lines mark distances typically traversed by the two satellites within a 24-h period. The continent is ochre.

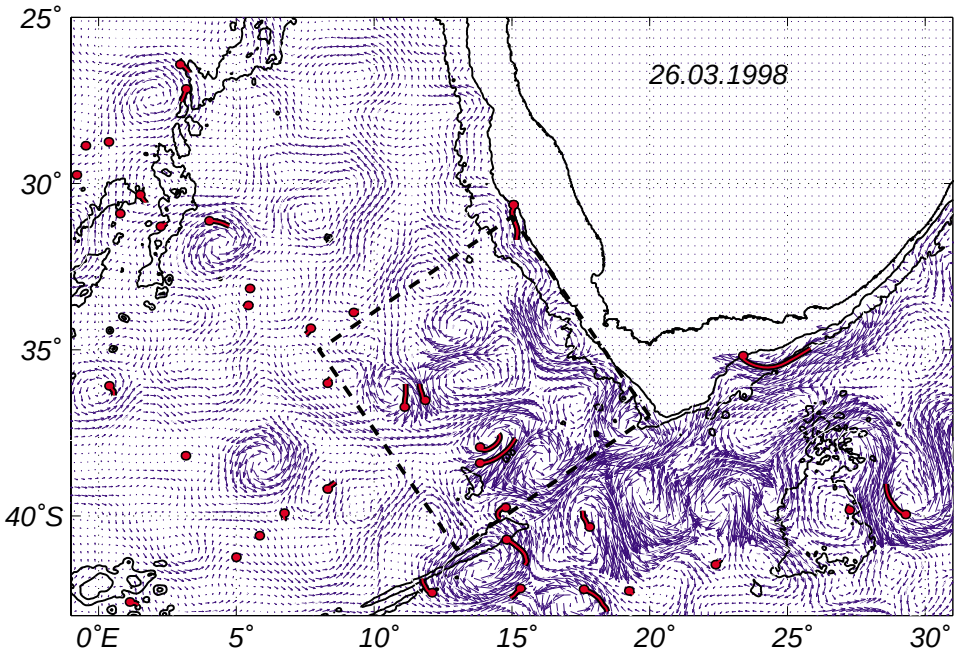

Fig. 3. Altimeter derived geostrophic velocity field (blue arrows) superposed by RAFOS float trajectory segments (red) representing 5 days of the floats drift. Each segment, consisting of head and tail, is centered on the nominal date of the satellite composite image. The 0, 1000 and 3000 m isobaths are indicated in black.

"$\langle\,\rangle_{ap}$" indicates an averaging over the several years of the altimeter data collection period. As more data are collected and included in MODAS upgrades, the durations represented by these averages increase.

MODAS-2D surface velocities were derived from the daily MODAS-2D SSH fields[4] assuming a geostrophic balance, with u and v being the resulting zonal and meridional velocity components (Fu and Chelton, 2001). For our region of interest, the MODAS-2D field's resolution corresponds to 14 km in the meridional and to 11 km (at 40°S) in the zonal direction. At this resolution, the formal mapping error of the MODAS-2D derived geostrophic velocities (Koblinsky et al., 1992; Blayo et al., 1997; Le Traon and Dibarboure, 1999; Ducet et al., 2000) varies between 8 and 35 cm s^{-1} away from the shelf with its uncertain steric height estimates, with longer baselines for the SSH gradient estimates resulting in smaller errors, as already noted by Zlotnicki et al. (1993).

2.2. RAFOS float data

Subsurface velocity data between 200 and 1350 m depth were collected in the ocean surrounding South Africa using neutrally buoyant RAFOS floats (Rossby et al., 1986) deployed under the auspices of the KAPEX program (Boebel et al., 1998). The data presented here focus on those floats that drifted within the Cape Cauldron (Boebel et al., 2003a), i.e. the southeastern part of the Cape Basin, and the Agulhas Return Current (Boebel et al., 2003b). A detailed description of the float deployments, data acquisition and tracking procedures are given in Boebel et al. (2000). Subsurface positions were obtained at either 12 or 24 h intervals and the associated meridional and zonal velocities were estimated from the tangent along spline functions for latitude and longitude data, respectively. The trajectories, with a few exceptions when unfavorable geometric situations between sound sources and floats were unavoidable, are estimated to be accurate within 10 km, while relative positions of successive data points are correct within approximately 2 km. This later error, representative of a worst-case scenario, translates in a maximum velocity error of order 2 cm s^{-1}, whereas float velocities are in general significantly above this value.

[4]MODAS-2D data can be accessed via http://www7320.nrlssc.navy.mil/altimetry.

2.3. ADCP data

R.V. *Polarstern* departed from Cape Town to Bremerhaven on 22 March 1997, collecting ADCP data along a zigzag track through the Cape Basin. Errors in the measured cross-track and along-track velocity component were estimated at ± 8 and ± 6 cm s^{-1}, respectively. Here we will focus on data collected during the first three days of the cruise, when the ship traversed the Cape Cauldron, including a recently spawned Agulhas Ring. Schmid et al. (2003) (their Fig. 4) shows a superposition of the relevant MODAS-2D SSH field with the corresponding ADCP vector data (25–50 m bin). Gaps in the ADCP data are due to technical problems and the rejection of bad data.

Half a year later, hull mounted-ADCP sections were collected aboard the R.V. *Seward Johnson* cruise 97/04 (Boebel et al., 2000). The cruise departed Cape Town on 23 August 1997 to the southeast, across the Agulhas and Agulhas Return Current, then east towards the Agulhas Plateau and finally back northwest, reaching the South African coast on 31 August 1997. This cruise resulted in 2 ADCP sections across the Agulhas Current and 4 across the Agulhas Return Current. A visualization of the cruise track and ADCP data is given in Boebel et al. (2003b), their Fig. 3. For this analysis, the ADCP's 25–75 m depth bin was selected for all sections, with data points estimated at 30 min intervals while steaming.

3. Data comparison

Our primary intent is to understand whether the location and dimension of mesoscale oceanographic features, i.e. of an eddy or a meander, are depicted correctly by MODAS-2D. If this were the case, we could reliably derive eddy and

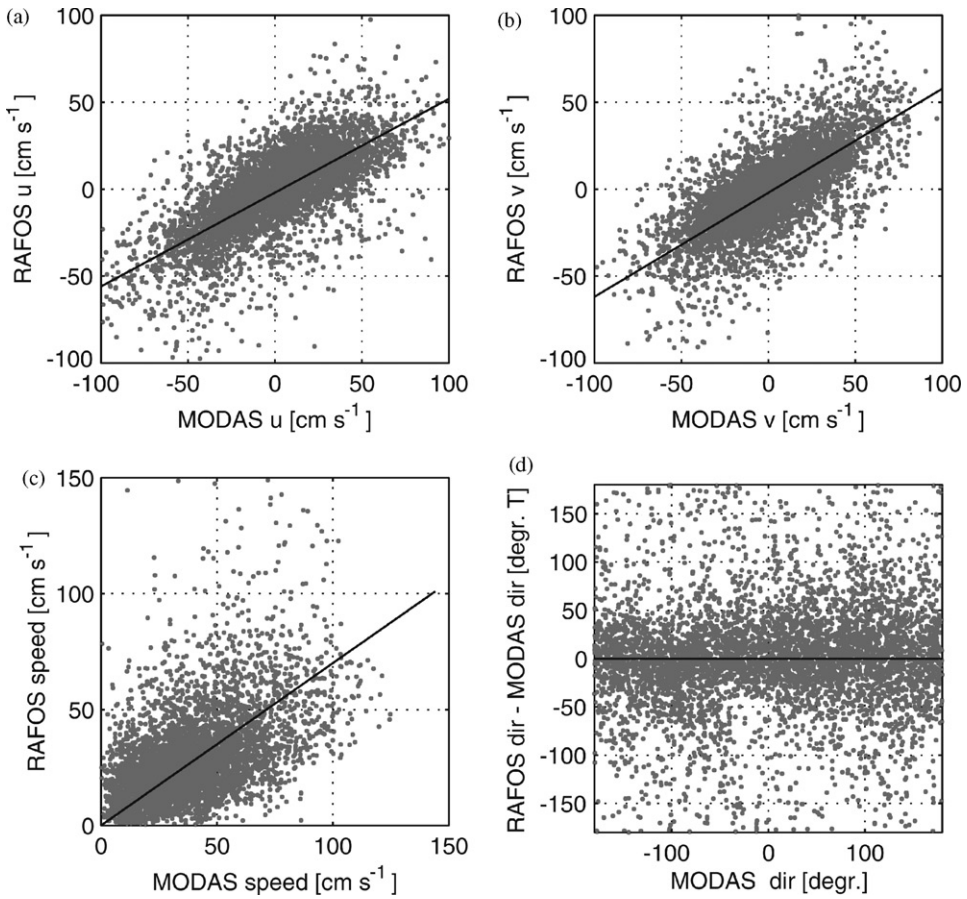

Fig. 4. Scatter plots from the Cape Cauldron region of subsurface RAFOS float velocities versus geostrophic surface velocities from MODAS-2D SSH: (a) zonal and (b) meridional velocity components; (c) speed; (d) angular difference between MODAS-2D and RAFOS velocity vectors versus the direction of the MODAS-2D velocity vectors. Black lines (panels (a)–(c)) indicate results from a least-square fit, which was forced to $v_{\mathrm{RAFOS}} = 0$ cm s^{-1} at $v_{\mathrm{MODAS\text{-}2D}} = 0$ cm s^{-1} for panel (c) (speed). In panel (d) the $\Delta\alpha = 0$ line is indicated. Regression parameters and correlation coefficients are given in Table 1.

meander properties from MODAS-2D as well as interpret in-situ point measurements in the wider oceanographic context. In particular, one could monitor the shedding and propagation of Agulhas Rings and smaller eddies, issues of significant interest to the oceanographic community. It is, however, a tedious exercise to try to extract the descriptive parameters of mesoscale features, such as propagation speed and diameter of an eddy, from the two measurement systems. The derivation of such data, for example from trajectories of individual floats, would in itself be prone to error due to the subjectivity of several assumptions necessary in such calculations.

Alternatively, a direct, day-by-day comparison of the float velocities with the associated simultaneous and co-located MODAS-2D geostrophic velocities over an extended period of time promises insight into the trustworthiness of the MODAS-2D SSH field. If we can show that the day-by-day velocity fields compare well in a statistical sense, it then appears appropriate to assume that the evolution from one state to the other is well represented too. This in turn implies that the

evolution of an individual mesoscale signal is likely to be depicted correctly as well.

Of particular interest to us is the correlation between the flow *directions* of geostrophic and subsurface in-situ velocities below the Ekman layer, which have little susceptibility to wind induced drifts. While baroclinic shear will lead to a decorrelation of surface and subsurface speeds, the flow directions are likely to correlate better, particularly in the presence of strong coherent mesoscale signals.

However, a regional dependency of the correlation between surface and subsurface data cannot be excluded. In particular, regions with a strong mean flow, such as the Agulhas Current or the Agulhas Return Current, need to be distinguished from regions of smaller mean kinetic energy (MKE). This is due to the addition of the climatological steric height anomaly field (Eq. (2)), which becomes significant for regions of strong MKE.

3.1. MODAS-2D versus RAFOS in the Cape Cauldron

The Cape Cauldron is characterized by strong mesoscale variability, which, in the past, has mostly been attributed to the shedding of Agulhas Rings (Le Traon and Morrow, 2001). KAPEX however, revealed that cyclonic eddies are of equal prominence in this region (Boebel et al., 2003a). These cyclones, together with Agulhas Rings, manifest themselves in alternating mesoscale patches of positive and negative sea-surface height anomalies. The height difference between maximal and minimal elevations is well above 1 m, reaching up to 2 m in extreme situations. This results in an intense mesoscale flow field with surface total kinetic energies of 59 J m^{-3} (Boebel et al., 2003a).

Scatter plots of subsurface RAFOS float velocities versus MODAS-2D derived geostrophic surface velocities are shown in Fig. 4. The comparison is restricted to the Cape Cauldron, i.e. the dashed box in Fig. 3, with corners at 37°S 20°E; 31°S 15°E; 35°S 8°E and 41°S 13°E. Panels (a) and (b) of Fig. 4 depict the zonal and meridional velocity components. Panel (c) shows speed while (d) depicts the angular difference ($\Delta\alpha$) between MODAS-2D and RAFOS velocities versus the direction of the MODAS-2D velocity. Linear fits (black lines in Fig. 4, panels (a)–(c) were performed according to

$$v_{\mathrm{RAFOS}} = \mathrm{slope} \cdot v_{\mathrm{MODAS\text{-}2D}} + \mathrm{offset}. \quad (3)$$

Bootstrapping the samples 1000 times (Emery and Thomson, 1997) and calculating of the 95-percentile interval of the resulting parameter arrays yields the error estimates given in Table 1.

Zonal and meridional slopes of 0.53 and 0.60 were obtained for the zonal and meridional component, respectively. Average subsurface speeds at intermediate depth amount to a fraction of 0.69 of the surface value. Offsets at $v_{\mathrm{MODAS\text{-}2D}} = 0$ cm s^{-1} are of little significance for either velocity component. The relative angle between RAFOS float and MODAS-2D geostrophic velocity (panel (d)) lacks a significant trend or offset, suggesting a co-directed flow of the two velocity fields. A histogram (not shown) of the $\Delta\alpha$ distribution peaks near $\Delta\alpha = 1^\circ$ with near symmetric lobes on the anti-cyclonic and cyclonic sides. The standard deviation of $\Delta\alpha$ amounts to $\pm 55^\circ$ and the 95-percentile interval to $\pm 130^\circ$.

The correlation coefficients for zonal and meridional speed ($r \approx 0.71$) suggest that about half of the observed variance is explained by linear regression. A significantly higher correlation coefficient of $r = 0.89$ is found for the directional comparison. The rms difference between geostrophic and in-situ velocity components is 19 cm s^{-1}, while the internal rms variability from float data is around 14 and 25–27 cm s^{-1} for MODAS. The values lie at the lower limit of the intrinsic intermediate depth rms variances observed by Eulerian current meters moored at near the southern boundary of the Cape Cauldron. Based on MKE and EKE published by Schmitz (1996) we estimate rms values ranging between 28 cm s^{-1} (instrument 8342A at 741 m depth) and 18 cm s^{-1} (instrument 8343B at 1493 m depth).

3.2. MODAS-2D versus RAFOS in the Agulhas Return Current

A completely different oceanic regime is found near the Agulhas Return Current. This current

Table 1
Regression parameters and correlation coefficients (v_{RAFOS} = slope $v_{MODAS\text{-}2D}$ + offset) for a comparison of MODAS-2D geostrophic velocities with RAFOS float subsurface velocities in the Cape Cauldron region

	Zonal	Meridional	Speed	Relative angle ($\Delta\alpha$)
	(a) *Unrestricted* (*5598 points*; *39 floats*)			
Slope	0.53 ± 0.02	0.60 ± 0.02	0.69 ± 0.01	—
Offset (cm s^{-1})	-0.8 ± 0.4	-0.5 ± 0.4	—	$1.2^\circ\pm1.5^\circ$
Correlation coefficient	0.70 ± 0.02	0.72 ± 0.01	0.52 ± 0.03	0.89 ± 0.01
rms (difference)	20.0 cm s^{-1}	18.4 cm s^{-1}	19.5 cm s^{-1}	52.6°
	(b) *Above* 800 m (*3369 points*; *33 floats*)			
Slope	0.57 ± 0.03	0.65 ± 0.03	0.77 ± 0.02	—
Offset (cm s^{-1})	-0.5 ± 0.6	-0.9 ± 0.6	—	$2.4^\circ\pm2.1^\circ$
Correlation coefficient	0.67 ± 0.02	0.70 ± 0.02	0.52 ± 0.03	0.88 ± 0.01
	(c) 800–1000 m (*1796 points*; *17 floats*)			
Slope	0.48 ± 0.02	0.52 ± 0.02	0.56 ± 0.02	—
Offset (cm s^{-1})	-0.3 ± 0.4	-0.4 ± 0.4	—	$0.9^\circ\pm1.9^\circ$
Correlation coefficient	0.81 ± 0.02	0.79 ± 0.03	0.59 ± 0.03	0.92 ± 0.01
	(d) *Below* 1000 m (*412 points*; *13 floats*)			
Slope	0.45 ± 0.03	0.42 ± 0.03	0.49 ± 0.02	—
Offset (cm s^{-1})	-3.7 ± 0.8	0.2 ± 0.7	—	$1.3^\circ\pm4.7^\circ$
Correlation coefficient	0.85 ± 0.03	0.80 ± 0.04	0.68 ± 0.05	0.89 ± 0.02

The 95-percentile interval is included as error estimate and based on bootstrapping the samples 1000 times. Root-mean-square values of differences between geostrophic and in-situ velocities are given in the last row of each block.

exhibits a quasi-stationary meandering pattern, with a rather stable zonal position between 38°S and 40°S (Boebel et al., 2003b). This results in most of the cross-current SSH variation being carried by the climatological (mean) altimetric field, while the SSH anomaly field lacks a noticeable mean zonal flow. Much of the meridional SSH gradient depicted by MODAS-2D and exemplified in Fig. 1 is therefore due to Eqs. (2b) and (2c).

The accompanying publication by Boebel et al. (2003b) develops a scheme to extract float trajectory segments that are likely to represent the Agulhas Return Current, excluding local recirculations or neighboring eddies. After a first visual extraction of data, two independent criteria are applied. First, only float data with speed exceeding 10 cm s^{-1} are retained. Second, each associated float pressure and temperature duplet is required to fall within a predefined property space characteristic for the ARC. Building on this selection of ARC float data, the resulting scatter plots of subsurface (RAFOS) versus surface (MODAS) velocities are presented in Fig. 5.

Linear regressions of the data result in the *slope* and *offset* coefficients as given in Table 2. The *slope*s of the velocity components are smaller (0.36 and 0.53) in comparison with the respective results for the Cape Cauldron. The independently fitted speed *slope* suggests that only a fraction of 0.55 of the surface speed is retained at the intermediate depth. Zonal float velocities are significantly offset by $+7.8$ cm s^{-1} (eastward) with respect to the MODAS-2D velocities, while no such offset exists either for the ARC meridional component or for the Cape Cauldron data. A test whether the observed offset could be due to our selection of 10 cm s^{-1} as a minimum speed for accepting float data to the ARC float data set was performed by changing the cut-off value to 0 cm s^{-1} instead. This control experiment produced similar offsets as above, in rejection of such hypothesis.

A preferred angular segment is observed for this region (Fig. 5, panel (d). Since the ARC data are

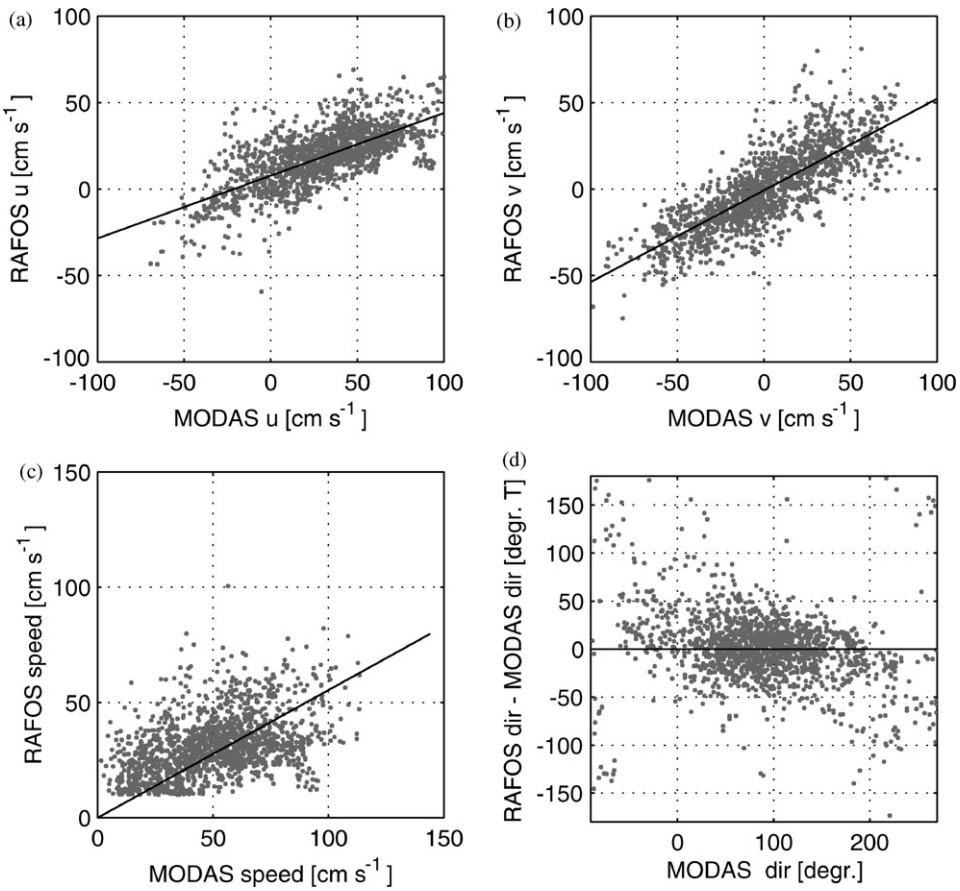

Fig. 5. Scatter plots in the ARC region of subsurface RAFOS float velocities versus geostrophic surface velocities from MODAS-2D SSH: (a) zonal and (b) meridional velocity components; (c) speed; (d) angular difference between MODAS-2D and RAFOS velocity vectors versus the direction of the MODAS-2D velocity vectors. Black lines (panels (a)–(c)) indicate results from a least-square fit, which was forced to $v_{\mathrm{RAFOS}} = 0$ cm s^{-1} at $v_{\mathrm{MODAS\text{-}2D}} = 0$ cm s^{-1} for panel (c) (speed). In panel (d) the $\Delta\alpha = 0$ line is indicated. Regression parameters and correlation coefficients are given in Table 2. Note that one of the conditions for the selection of ARC RAFOS data was speed > 10 cm s^{-1}, which is reflected in the cut-off velocity visible in panel (c).

collected from within a quasi-zonal eastward current, the clustering around MODAS-2D direction = 90° is reasonable. The data furthermore suggest negative relative angles $\Delta\alpha$ for MODAS-2D velocity directions east (90°) to south (180°), while positive relative angles $\Delta\alpha$ are observed for MODAS-2D data in the quadrant North (0°) to east (90°). With the relative angle $\Delta\alpha$ calculated as RAFOS direction minus MODAS-2D direction, this implies that the RAFOS directions tend to point more to the East than the MODAS-2D velocities. This appears to be a direct consequence of the abovementioned eastward velocity offset observed in the meridional velocity scatter plot. The high correlation between RAFOS and MODAS-2D directions is reflected in a narrow directional frequency distribution (not shown) with a standard deviation of $\pm 38°$, while the 95-percentile intervals equals to $\pm 87°$. The mean difference of $\Delta\alpha$ equals 1°.

A high correlation coefficient (0.83) is observed for the relative angle $\Delta\alpha$, paired with significant correlation (0.70 and 0.79) coefficients for zonal and meridional velocities. The rms differences between geostrophic and in-situ velocity components scatter around 24 cm s^{-1}. Internal rms

Table 2
Correlation and linear regression (v_{RAFOS} = slope $v_{MODAS\text{-}2D}$ + offset) coefficients for a comparison of ARC RAFOS float velocities and corresponding MODAS-2D velocities

	Zonal	Meridional	Speed	Relative angle ($\Delta\alpha$)
	(a) *Unrestricted* (*1522 points*; *15 floats*)			
Slope	0.36±0.02	0.53±0.02	0.55±0.01	—
Offset (cm s^{-1})	**7.8±1.0**	−0.7±0.7	—	1.0±2.0
Correlation coefficient	0.70±0.03	0.80±0.02	0.44±0.04	0.83±0.03
rms (difference)	25.9 cm s^{-1}	21.3 cm s^{-1}	28.2 cm s^{-1}	39.9°
	(b) *Above* 800 m (*401 points*; *10 floats*)			
Slope	0.52±0.05	0.63±0.05	0.69±0.03	—
Offset (cm s^{-1})	**4.5±2.0**	−0.2±1.5	—	−2.9±3.6
Correlation coefficient	0.75±0.05	0.83±0.04	0.66±0.06	0.88±0.03
	(c) 800–1000 m (*808 points*; *13 floats*)			
Slope	0.38±0.03	0.53±0.02	0.58±0.02	—
Offset (cm s^{-1})	**8.9±1.1**	−1.4±0.9	—	2.8±2.8
Correlation coefficient	0.73±0.04	0.81±0.02	0.52±0.05	0.80±0.04
	(d) *Below* 1000 m (*313 points*; *4 floats*)			
Slope	0.23±0.04	0.38±0.04	0.40±0.02	—
Offset (cm s^{-1})	**9.0±2.3**	0.3±1.2	—	1.3±3.7
Correlation coefficient	0.67±0.10	0.77±0.04	0.01±0.12	0.82±0.04

Included errors are based on the 95-percentile interval, which was estimated by bootstrapping the sample 1000 times.

Table 3
Correlation and regression coefficients between ADCP (25–50 m bin) and MODAS-2D velocities for the Cape Cauldron region

167 data duplets	Zonal	Meridional	Speed	Relative angle ($\Delta\alpha$)
Slope	1.04±0.08	0.18±0.26	1.11±0.07	—
Offset (cm s^{-1})	−0.1±3.5	−9.8±3.2	—	25.5°±12.1°
Correlation coefficient	0.90±0.03	0.11±0.16	0.84±0.06	0.27±0.17
rms (difference)	20.2 cm s^{-1}	24.6 cm s^{-1}	19.9 cm s^{-1}	125.8°

Error estimates are based on the 95-percentile interval, estimated by bootstrapping the array 1000 times (Emery and Thomson, 1997).

variance estimates from the float data are between 17 and 23 cm s^{-1}, from MODAS-2D velocities 32–34 cm s^{-1}. These values lie amidst the range of the intrinsic intermediate depth rms variances observed by Eulerian current meters moored in the vicinity of the ARC. Based on the Schmitz (1996) MKE and EKE estimates we calculate a rms range of 17 cm s^{-1} (instrument 8343B, 760 m depth) to 30 cm s^{-1} (instrument 8372A, at 841 m depth).

3.3. MODAS-2D versus ADCP

In the following we will compare the KAPEX ADCP data with co-located MODAS-2D data. The two sections, due to their location, distinguish between the Cape Cauldron and Agulhas Return Current regions, with the inclusion of some data from the Agulhas Current proper in the later data set.

For each ADCP data point obtained west of 11°E and north of 43°S during R.V. *Polarstern* cruise ANT-XIV, the corresponding co-located MODAS-2D velocity was estimated. Scatter plots (not shown) were produced and correlation coefficients and regression parameters calculated. The comparison (Table 3) yields a high zonal correlation coefficient ($r = 0.90$). However, the correlation coefficient for the meridional

component is not significantly different from zero. The decomposition of the vector velocity into speed and direction indicates a good correlation for speed, while the directional correlation is low. This reflects the poor match in the meridional component, which produces a large scatter in relative angles. A near perfect regression (slope ≈ 1) is observed for the zonal component while the result is insignificantly different from zero for the meridional part. The rms difference between ADCP and geostrophic velocities ranges between 20 and 25 cm s^{-1}, significantly below the inherent zonal ADCP and MODAS-2D rms variability of 40 and 46 cm s^{-1}, but slightly above the meridional values (12 and 19 cm s^{-1}). In comparison, the natural near-surface variability in this region derived from a single current meter at 195 m depth is 54 cm s^{-1} (instrument 8381B, (Schmitz, 1996)).

A greater consistency of zonal and meridional MODAS-2D and ADCP velocities is observed in the ARC region. The resulting correlation coefficients (Table 4) are 0.79 (zonal) and 0.64 (meridional), with the zonal component somewhat better correlated than the meridional component. The linear regression parameter slope approximates 1 within its error limits for both components, as does the regression for speed. The rms difference between ADCP and geostrophic velocities varies from 27–42 cm s^{-1}, overlapping with the range of the intrinsic near-surface variability from MODAS-2D (27–38 cm s^{-1}) and close to 31 cm s^{-1} derived from a single current meter in this region at 210 m depth (instrument 8421A, (Schmitz, 1996)). The rms difference is however significantly lower than the intrinsic rms ADCP velocity variance of 44–50 cm s^{-1}.

Comparing data duplet by data duplet in the Cape Cauldron data set (Fig. 6) confirms the good agreement for the zonal component, in particular for the part across the Agulhas Ring (data points 20–60). The section traversed the ring from north to south, passing the ring's center closely (see Schmid et al. (2003, their Fig. 4)). The geometry explains the dominance of the zonal flow component at the ring's northern and southern perimeter. The zonal ADCP and MODAS-2D data agree in intensity (both peak around 100 cm s^{-1}) and phase, while geostrophic cross-section velocity estimates based on the concurrent hydrographic section referenced to 1600 m are lower (60 cm s^{-1}) (Schmid et al., 2003). The subsequent westward leg shows a decreasing agreement between ADCP and MODAS-2D, with the ADCP data showing more sub-mesoscale structure.

As already indicated by the statistical results, the meridional velocity correlation is severely reduced. Within the rings perimeter, the ADCP signal phase appears to lag the MODAS-2D signal by order of 10 data points or the equivalent of 55 km. MODAS-2D and ADCP peak amplitudes (50 cm s^{-1}) for this data segment differ by about 20 cm s^{-1}. Data duplets past data point 80 are devoid of any significant correlation, with the ADCP signal showing a strong sub-mesoscale field, while the MODAS-2D signal oscillates around zero.

The point-by-point comparison of ARC data (Fig. 7) shows, relative to the ADCP data, a smoothed MODAS-2D derived velocity field. The amplitude (or maximum velocity) observed in the MODAS-2D data is comparable to the zonal ADCP component, but differs markedly for the

Table 4
Correlation and regression coefficients between ADCP (25–75 m bin) and MODAS-2D velocities for the ARC region

ARC (142 data duplets)	Zonal	Meridional	Speed	Relative angle ($\Delta\alpha$)
Slope	0.98 ± 0.18	1.19 ± 0.22	1.30 ± 0.17	—
Offset (cm s^{-1})	-1.8 ± 5.5	17.6 ± 6.7	—	-10.2 ± 11.1
Correlation coefficient	0.79 ± 0.09	0.64 ± 0.12	0.63 ± 0.11	0.64 ± 0.14
rms (difference)	27.2 cm s^{-1}	42.5 cm s^{-1}	36.8 cm s^{-1}	78.7°

The correlation coefficients are calculated using data points 40–180 from Fig. 7. Error estimates are based on the 95-percentile interval, estimated by bootstrapping the array 1000 times (Emery and Thomson, 1997).

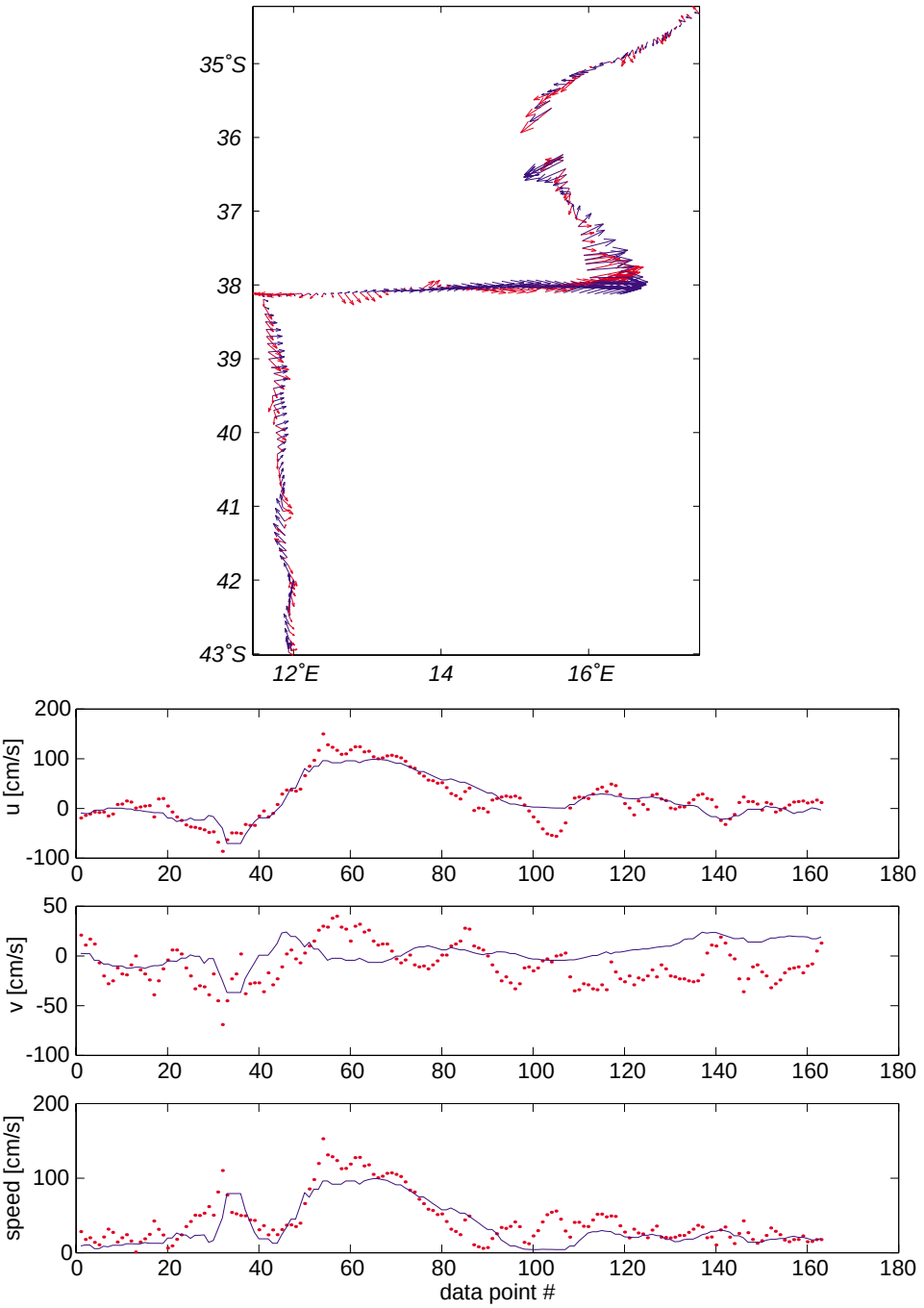

Fig. 6. Top: Cape Cauldron ADCP velocity vectors (25–50 m depth) from R.V. *Polarstern* cruise ANT XIV (red) versus concurrent surface velocities estimates from MODAS-2D (blue). Bottom: The *u*- and *v*-components as well as speed. The abscissa does not linearly relate to physical properties such as time or distance, but gives the linearly increasing number of valid ADCP/MODAS-2D data duplets.

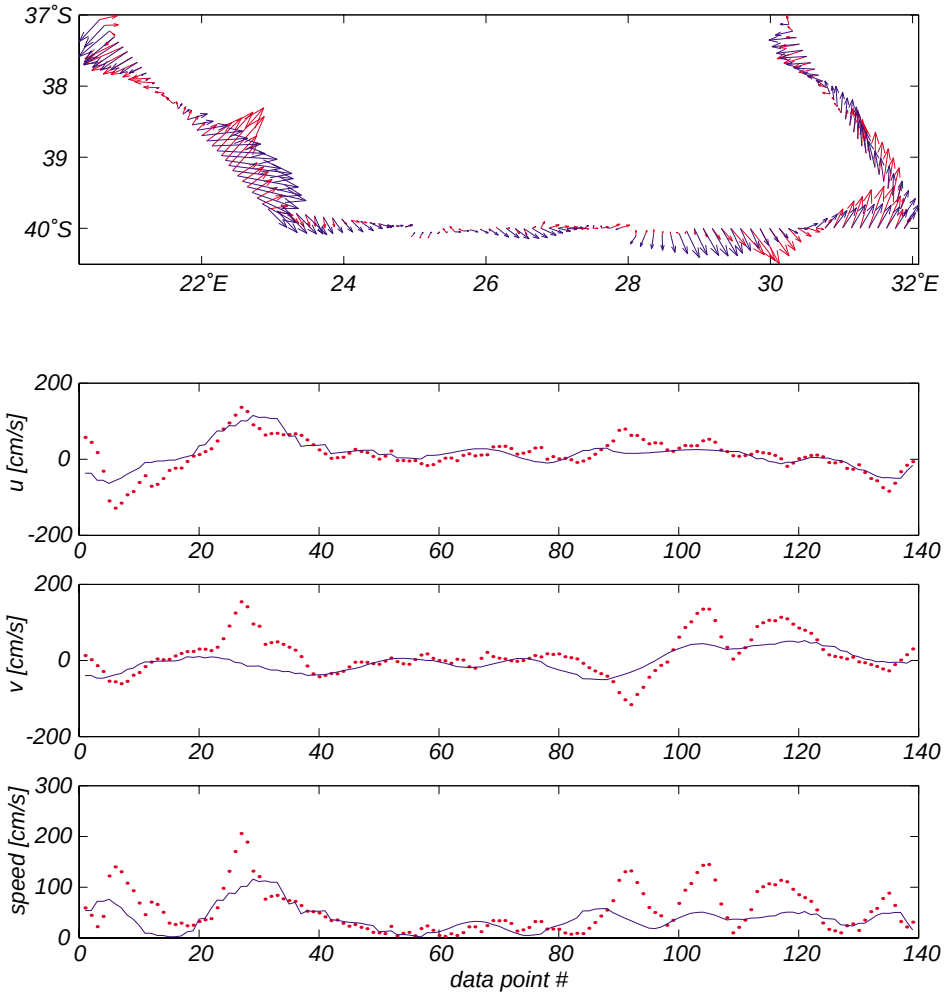

Fig. 7. Top: Agulhas Return Current ADCP velocity vectors (25–75 m depth, red) versus concurrent surface velocities estimates from MODAS-2D (blue). Bottom: The u- and v-components as well as speed. The abscissa does not linearly relate to physical properties such as time or distance, but gives the linearly increasing number of valid ADCP/MODAS-2D data duplets. ADCP/MODAS-2D data duplets were included only if the ship steamed at a minimum speed of 8 knots and if a MODAS-2D speed estimate was possible, that is, in waters deeper than 1000 m. Data from the ARC region lie between data points 40 and 180.

meridional components. Two occasions are noteworthy herein:

(a) The strong northward component of the ARC west of the Agulhas Plateau (Fig. 7, data points 20–30) is missed. While MODAS-2D captures near zero meridional velocity, the ADCP peaks at 150 cm s^{-1}. The zonal component of similar intensity is however captured correctly both in phase and amplitude.

(b) The repeated crossings of the ARC's first crest (Fig. 7, data points 80–90) are captured with reduced amplitude (the difference amounts to 50 cm s^{-1} or half the ADCP signal). The first crossing is positioned farther west and appears broader in MODAS-2D than in the ADCP data. However, the subsequent zero crossing of the meridional velocity component (that is the transition from the approaching to the receding branch of the ARC, see Boebel

et al. (2003b), their Fig. 3) is in close proximity for the two data sets (near data point 100).

4. Discussion

Both the RAFOS/MODAS-2D and ADCP/MODAS-2D comparisons provided encouraging results. While the comparison between MODAS-2D derived—and ADCP velocities yielded the regression coefficients with slope ≈ 1 (except for one outlier), the corresponding correlation coefficients were less significant. Contrastingly, the RAFOS/MODAS-2D directional comparison yielded high correlation coefficients, while the slopes between the MODAS-2D surface and the RAFOS subsurface velocities lie between 0.5 and 0.8. An offset was observed for the zonal Agulhas Return Current data, but not for the meridional ARC component or for the Cape Cauldron data.

These results are not unexpected. While the comparison of surface velocities (i.e. ADCP and MODAS-2D) should provide comparable amplitudes, their directions might vary mostly due to the influence of the wind driven Ekman currents. Comparing RAFOS with MODAS-2D data, on the other hand, avoids the wind's influence in both data sets, but is subject to the baroclinic velocity shear as a source of difference. This is manifested in the high RAFOS/MODAS-2D correlation coefficients in conjunction with the lower slope values of the linear regressions.

4.1. Ageostrophic and mapping errors

An obvious source for such discrepancy between geostrophic MODAS-2D and in-situ velocities are geographic restrictions of the climatological field used in MODAS. In the ARC MODAS-2D/ADCP comparison, we noted that the Agulhas Current off Port Elizabeth is missed in the MODAS-2D field altogether. (This particular part of the comparison lies north of the area depicted in Fig. 7). The mismatch is explained by the cutoff of the MODAS-2D field at the 1000 m isobath. When the Agulhas Current is found at or inshore of the 1000 m line, the mapping procedure, using mesoscale correlation lengths, will fail to depict the current properly. Choosing the 500 m level as reference, rather than 1000 m, could alleviate this particular problem. However, in the open ocean other sources of must be responsible for differences between MODAS-2D and ADCP velocities.

Given the scarcity of additional data from this part of the oceans, the discussion of these errors must rely on previous dedicated studies from other regions. Possible, but less palpable error sources are discussed by Strub et al. (1997) in their study of in-situ and altimetric data within the California Current System. Both near-inertial motions and internal waves are listed as cause for differential ADCP and geostrophic velocities. Strub et al. (1997) point out that near-inertial motions are contained in the altimeter heights as measured by the satellites and result in a typical velocity signal of 2–4 cm s^{-1}. D'Asaro et al. (1995) report mesoscale varying signal strengths of 10 cm s^{-1} due to inertial motions, providing an upper limit of the error to be expected from this source. The MODAS-2D mesoscale mapping will spread this signal over the respective correlation radius. The signal's impact on the overall velocity field, however, will depend significantly on the pattern of neighboring (in space and time) SSH signals. The unfiltered high resolution ADCP data on the other hand will resolve the inertial signal (the inertial period is about 21 h around southern Africa). A similar situation exists for internal waves, which are likely to alias the MODAS-2D data, while ADCP data could resolve this component.

A third source of contamination of the geostrophic velocity signal is the wind-driven Ekman current. This signal would not be part of the derived altimetric velocities. However, depending on sampling and thermocline depth, the signal could show up in the ADCP data. The ADCP data used herein were collected from the 25–75 m bin. Using this depth bin rather than those above or below resulted in the highest correlation with MODAS-2D velocities, but nevertheless is likely to bear contamination from the Ekman signal.

To explain the entire observed discrepancy of up to 50 cm s^{-1}, however, we need to amend this list

by another culprit. Based on our observation of several events of phase differences between MODAS-2D and ADCP signal, particularly for the meridional component, the objective analysis process involved in the MODAS-2D generation is suspected of introducing errors. Mismatches in phase might be due to mismatch in the timescales at which MODAS-2D can adjust to changes and those at which they occur in the real ocean. The time lag between subsequent satellite passes (10 days for TOPEX/POSEIDON and 35 days for ERS-2) and the correlation scales used in the objective analysis scheme when calculating the SSH field may conspire to make signals propagate or morph less rapidly than in reality. The formal mapping error of MODAS, as high as 30 cm s^{-1} for data in between tracks, is an expression of this uncertainty. After all, both regions are not only characterized by high particle velocities, which should facilitate the satellite measurements, but also by rapid changes in the overall field, with feature phase velocities of up to 30 cm s^{-1}, i.e. larger than the observed rms difference in the comparisons. Solid black lines in Fig. 2 give an impression of the distance that is actually traversed by the two satellites in a 24-h period, leaving large gaps in between that need to be filled in by the objective mapping scheme of MODAS-2D. Individual features can be expected to appear less intense and broader than in reality (smearing). Their position might be offset by limited distances (shifting), which, in agreement with the data presented here, have been shown to be shorter than the correlation scales involved (80–100 km) (Jacobs et al., 2001). Analogous observations for the full 4-D MODAS field have been made in the Japan/East Sea (Fox et al., 2002). In their study Fox et al. (2002) proceeded to show that MODAS-2D would reproduce the observed horizontal variability in this region without shifting and smearing if provided with error free, synoptic SST and SSH data.

It is worth noting that misallocations of mesoscale features are not necessarily propagated past the satellite repetition period. The constant correction of the SSH anomaly through the input of new altimetric data into MODAS-2D will relocate a misplaced feature as soon as it is captured by the next overflight. Hence the propagation of phase signals at time scales longer than the repetition period is adequately sampled, as also shown in accompanying studies of propagating single eddies (Lutjeharms et al., 2003; Schmid et al., 2003) observed through MODAS-2D and by RAFOS floats trapped within.

4.2. Baroclinic errors

Our primary in-situ data source, the RAFOS floats, are, due to their 24-h sampling and greater floating depth, not subject to the ageostrophic contaminations discussed above. However velocity differences between MODAS-2D and RAFOS velocities are introduced by baroclinic shear. Grouping the RAFOS floats into different sets characterized by depth ranges (above 800 m, 800–1000 m and below 1000 m) amplifies this notion. Fig. 8a shows a systematic decrease of the *slope* parameter with depth for the combination of MODAS-2D/RAFOS and MODAS-2D/ADCP velocities. The directional correlation between RAFOS and MODAS-2D data varies between 0.8 and 0.9 (Fig. 9) and is independent of the depth selection, while the ADCP/MODAS-2D comparison (data labeled "surface") is rendered insignificant due to high error bars. Details of the resulting correlation and regression coefficients and their associated errors are included in Tables 1 and 2.

A separation into the three depth layers shows a limited depth dependence for the previously noted significant zonal offset of 7.8 cm s^{-1} between RAFOS and MODAS-2D ARC data (Fig. 8b). On the other hand, no significant offset is found for either the meridional ARC data, or for both the Cape Cauldron meridional or zonal offsets.

The assumption of a simple linear relationship between surface and subsurface velocities for various locations across a current or eddy is theoretically incorrect but practically useful. This is exemplified in Fig. 10 by plotting geostrophic co-located subsurface velocities versus surface velocities for a generic ARC section developed in Boebel et al. (2003b). The scatter plot depicts an elongated, quasi-linear beacon shaped cloud of data points. The variability in subsurface velocity,

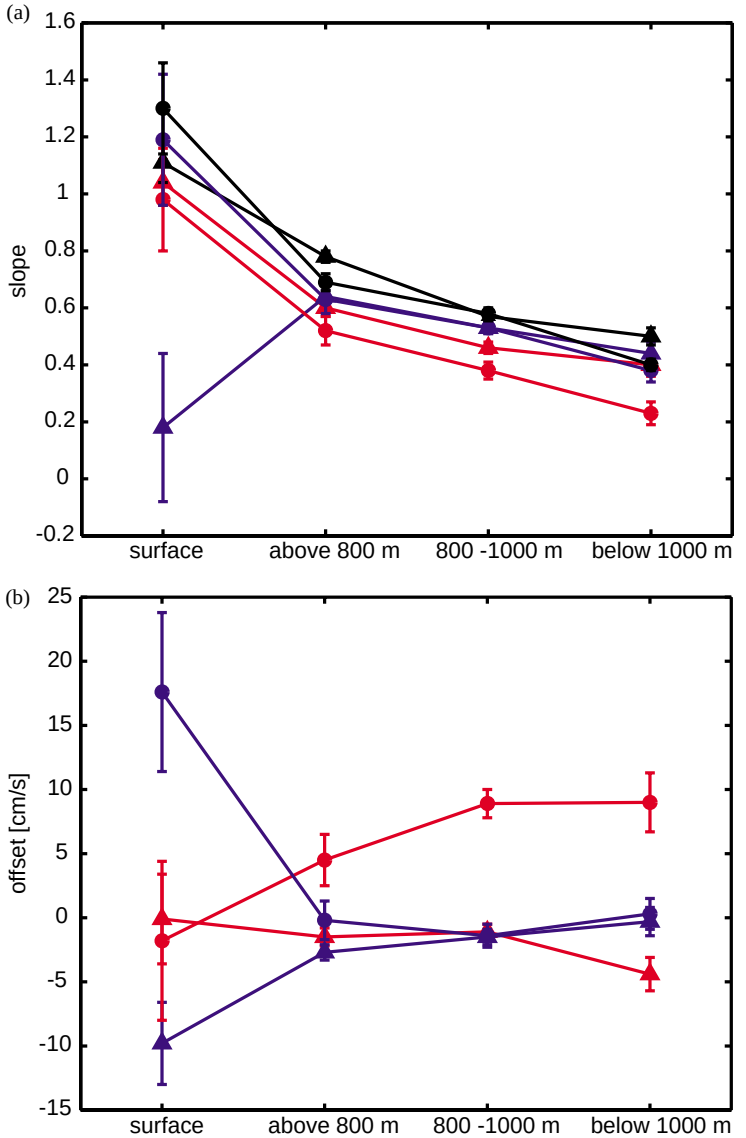

Fig. 8. Regression coefficients (slope, top and offset, bottom) for linear fits of zonal (red) and meridional (blue) velocities of MODAS-2D versus ADCP (labeled "surface") and MODAS-2D versus RAFOS (labeled "above 800 m", "800–1000 m", and "below 1000 m"). Black symbols/lines in the slope panel indicate results for speed. Triangles mark results for the Agulhas Return Current region, while dots indicate results for the Cape Cauldron. See Tables 1–4 for further details.

for a given surface velocity stems from the baroclinic shear across the chosen depth interval. In this example, the plot shows three beacons, formed by selecting specific depth ranges: (a) 100–300 m (top), (b) 500–700 m (middle) and, (c) 900–1100 m (bottom). As to be expected, with increasing depth, the linear regression coefficient between surface and subsurface velocities decreases. With our depths bins chosen contiguous, the superposition of such beacons is partly responsible for the wide scatter visible in Figs. 4 and 5.

However, an important parameter can be extracted by fitting a straight line to the data, regardless if the data is grouped together or

separated according to depth intervals. The barotropic velocity might only partially be contained in the MODAS-2D derived surface velocities, due to the later being referenced to a level of presumably zero, but in fact unknown, speed. In the RAFOS/MODAS-2D velocity scatter plots, such incomplete representation would reveal itself in a depth invariant offset $v_{\text{subsurface}} \neq 0$ m s^{-1} at $v_{\text{surface}} = 0$ m s^{-1}. This situation is illustrated in Fig. 10 by adding 0.1 m s^{-1} to the subsurface velocity data only. Clearly, an offset to all three beacons becomes visible in the simulation.

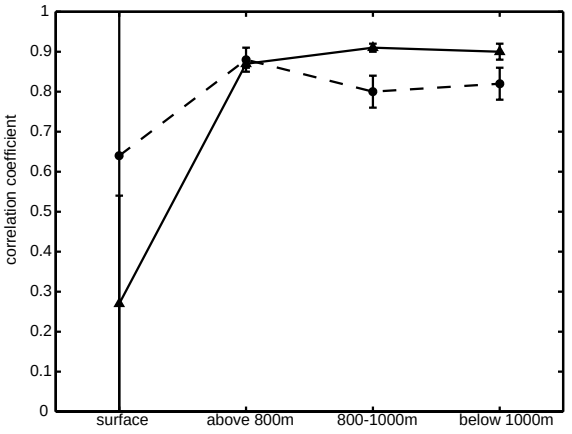

Fig. 9. Directional correlation coefficients for the MODAS/ADCP (labeled "surface") and 3 groups of MODAS/RAFOS comparisons (labeled "above 800 m", "800–1000 m" and "below 1000 m"). Triangles mark results for the Agulhas Return Current region, while circles indicate results for the Cape Cauldron. See Tables 1–4 for further details.

In fact, the scatter plot and linear fits of the real RAFOS/MODAS-2D zonal ARC velocities indicate such offsets, varying between 5 and 10 cm s^{-1}. Hence we surmise that an additional zonal velocity component of this magnitude is present in the ARC at the reference level and above (Fig. 8b), and is currently missed in the MODAS-2D calculations. Contrastingly, no such observations are made for the meridional ARC and both Cape Cauldron velocity diagrams.

4.3. Final remarks

The comparison of daily, altimetry derived velocity fields with in-situ RAFOS velocities has proven a useful tool to independently quantify the aptness of remotely sensed, objectively

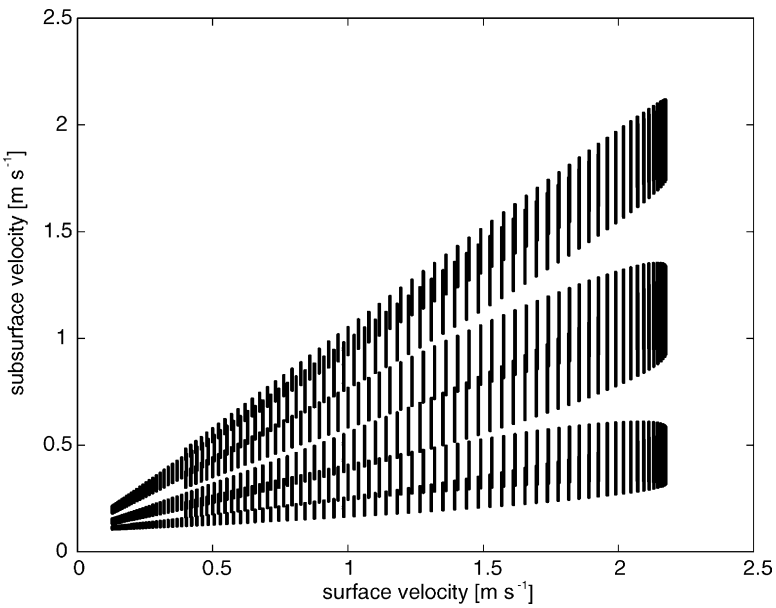

Fig. 10. Geostrophic subsurface—versus surface velocities of a current corresponding to the generic ARC section given in Boebel et al. (2003b). The three "beacons" correspond to selected depth ranges 100–300 m (top), 500–700 m (center), and 900–1100 m (bottom). Subsurface velocities were barotropically increased by 0.1 m s^{-1}.

interpolated surface velocity *fields*. It would be most interesting to extend this comparison in future studies to high-resolution data assimilating models or the full 4-D MODAS. Alternatively, one might try to examine in-situ and altimetric MODAS-2D velocities only for in-situ measurements located within a narrow space–time window of the satellites footprint to better understand the impact of the objective interpolation process. Last but not least, similar comparisons for other regions, particularly for the well-sampled North Atlantic would be of great value.

Nevertheless, this comparison of in-situ and MODAS-2D derived velocities around southern Africa suggests that the overall pattern of cyclonic and anticyclonic features as captured by daily MODAS-2D SSH fields is highly realistic and can therefore be used in an analysis of the phase propagation of these features. The observed rms difference of typically 25 cm s^{-1} is comparable to those observed for other highly energetic regions (Picaut et al., 1990). It can in parts be explained by the combined action of ageostrophic flow, baroclinic shear and the formal mapping error of MODAS-2D. The later reflects misallocations of mesoscale features due to the necessary MODAS-2D space–time interpolation and appears to be the major cause of uncertainty. Nevertheless, the MODAS-2D SSH field gives a reasonable approximation of the near surface velocity field in the Agulhas Return Current and Cape Cauldron regions, particularly when averaging over longer periods.

Acknowledgements

Excellent support through all officers and crews of vessels involved in KAPEX is greatly appreciated. These are, in alphabetical order, SA *KUSWAG I*, SA *KUSWAG V*, R.V. *Seward Johnson* and R.V. *Polarstern*. Further participants of KAPEX, i.e. Chris Duncombe Rae, Dave Fratantoni, Silvia Garzoli, Johann Lutjeharms, Phil Richardson, Tom Rossby, Claudia Schmid and Walter Zenk provided indispensable support and valuable scientific discussions throughout the project. Essential technical and scientific contributions were made by I. Ansorge, S. Becker, R. Berger, P. Bouchard, D. Carlsen, J. Fontaine, S. Anderson-Fontana, H. Hunt, J. Kemp, M. Nielsen and C. Wooding. We would like to thank Eric Firing, University of Hawaii, for the provision of ADCP data analysis software. Comments from two anonymous reviewers have been enormously helpful in condensing the paper to its present form. Support from the National Science Foundation, USA, the Foundation for Research Developments, RSA, the Ministerium für Bildung, Wissenschaft, Forschung und Technologie (Germany), the Alexander-von-Humboldt Foundation (Germany) and the Alfred Wegener Institut, Germany is acknowledged. MODAS-2D work is supported by the Oceanographer of the Navy via the Space and Naval Warfare Systems Command (SPAWAR) under program element 0603207N and the Northern Gulf Littoral Initiative (NGLI) program.

References

Blayo, E., Mailly, T., Barnier, B., Brasseur, P., Provost, C.L., Molines, J.M., Verron, J., 1997. Complementarity of ERS 1 and TOPEX/POSEIDON altimeter data in estimating the ocean circulation: assimilation into a model of the North Atlantic. Journal of Geophysical Research 102, 18,573–18,584.

Boebel, O., Duncombe Rae, C., Garzoli, S., Lutjeharms, J., Richardson, P., Rossby, T., Schmid, C., Zenk, W., 1998. Float experiment studies interocean exchanges at the tip of Africa. EOS 79 (1), 6–8.

Boebel, O., Anderson-Fontana, S., Schmid, C., Ansorge, I., Lazarevich, P., Lutjeharms, J., Prater, M., Rossby, T., Zenk, W., 2000. KAPEX RAFOS Float Data Report 1997–1999; Part A: The Agulhas- and South Atlantic Current Components. Institut für Meereskunde an der Christian-Albrechts-Universität-Kiel, Berichte aus dem Institut für Meereskunde 318, Kiel, pp. 194.

Boebel, O., Lutjeharms, J., Schmid, C., Zenk, W., Rossby, T., Barron, C., 2003a. The Cape Cauldron: a regime of turbulent interocean exchange. Deep-Sea Research II, this issue (PII: S0967-0645(02)00379-X).

Boebel, O., Rossby, T., Lutjeharms, J., Zenk, W., Barron, C., 2003b. Path and variability of the Agulhas Return Current. Deep-Sea Research II, this issue (PII: S0967-0645(02)00377-6).

Cheney, R.E., 1995. TOPEX/POSEIDON: scientific results. Journal of Geophysical Research 100, 24893.

D'Asaro, E.A., Eriksen, C.C., Levine, M.D., Niiler, P.P., Paulson, C.A., van Meurs, P., 1995. Upper-ocean inertial currents forced by a strong storm. I. Data and comparison

with linear theory. Journal of Physical Oceanography 25, 2909–2936.

Ducet, N., Le Traon, P.Y., Reverdin, G., 2000. Global high-resolution mapping of ocean circulation from TOPEX/Poseidon and ERS-1 and -2. Journal of Geophysical Research 105, 19477–19498.

Emery, W.J., Thomson, R.E., 1997. Data Analysis Methods in Physical Oceanography. Elsevier, Oxford, 634pp.

ESA, 2001. European Remote Sensing Satellites—ERS Home Page 2001.

Fox, D.N., Teague, W.J., Barron, C.N., Carnes, M.R., Lee, C.M., 2002. The Modular Ocean Data Assimilation System (MODAS). Journal of Atmospheric and Oceanic Technology 19 (2), 240–252.

Fu, L.-L., Christensen Jr., E.J., Lefebvre, C.A.Y.M., Menard, Y., Dorrer, M., Escudier, P., 1994. TOPEX/POSEIDON mission overview. Journal of Geophysical Research 99, 24369–24383.

Fu, L.-L., Chelton, D.B., 2001. Large-scale ocean circulation. In: Fu, L.-L., Cazenave, A. (Eds.), Satellite Altimetry and Earth Sciences. Academic Press, San Diego, CA, pp. 133–169.

Gill, A.E., 1982. Atmosphere–Ocean Dynamics. Academic Press, San Diego, CA, 662pp.

Jacobs, G.A., Barron, C.N., Rhodes, R.C., 2001. Mesoscale characteristics. Journal of Geophysical Research 106, 19581–19596.

Joyce, T.M., Kelly, K.A., Schubert, D.M., Caruso, M.J., 1990. Shipboard and altimetric studies of rapid Gulf Stream variability between Cape Cod and Bermuda. Deep-Sea Research A 37, 897–910.

Kelly, K.A., Beardsley, R.C., Limeburner, R., Brink, K.H., Paduan, J.D., Chereskin, T.K., 1998. Variability of the near-surface eddy kinetic energy in the California Current based on altimetric, drifter, and moored current data. Journal of Geophysical Research 103, 13,067–13,083.

Key, K.W., 1997. Theory and Applications of Using GPS Equipped Buoys for the Accurate Measurement of Sea Level. UMI, Ann Arbor, MI 48106, USA.

Koblinsky, C.J., Gaspar, P., Lagerloef, G., 1992. The Future of Spaceborn Altimetry: Ocean and Climate Change. Joint. Oceanogr. Inst. Inc., Washington, DC, 75pp.

Lagerloef, G.S.E., Mitchum, G.T., Lukas, R.B., Niiler, P.P., 1999. Tropical Pacific near-surface currents estimated from altimeter, wind, and drifter data. Journal of Geophysical Research 104, 23313–23326.

Le Traon, P.Y., Dibarboure, G., 1999. Mesoscale mapping of multiple-satellite altimeter missions. Journal of Atmospheric and Oceanic Technology 16, 1208–1223.

Le Traon, P.Y., Morrow, R., 2001. Ocean currents and eddies. In: Fu, L.-L., Cazenave, A. (Eds.), Satellite altimetry and earth sciences. Academic Press, San Diego, pp. 171–215.

Levitus, S., 1982. Climatological Atlas of the World Ocean. US Government Printing Office NOAA Professional Paper 13, Washington, DC, USA 173pp.

Lutjeharms, J.R.E., Boebel, O., Rossby, H.T., 2003. Agulhas cyclones, Deep-Sea Research II, this issue (PII: S0967-0645(02)00378-8).

Olbers, D., Gouretski, V., Seiß, G., Schröter, J., 1992. Hydrographic Atlas of the Southern Ocean. Alfred Wegener Institut, Bremerhaven, 82pp.

Picaut, J., Busalacchi, A.J., McPhaden, M.J., Camusat, B., 1990. Validation of the geostrophic method for estimating zonal currents at the equator from Geosat altimeter data. Journal of Geophysical Research 95, 3015–3024.

Rossby, T., Dorson, D., Fontaine, J., 1986. The RAFOS System. Journal of Atmospheric and Oceanic Technology 3, 672–679.

Schmid, C., Boebel, O., Zenk, W., Lutjeharms, J., Garzoli, S.L., Richardson, P.L., Barron, C.N., 2003. Early evolution of an Agulhas Ring. Deep-Sea Research II, this issue (PII: S0967-0645(02)00382-X).

Schmitz, W.J., 1996. On the eddy field in the Agulhas Retroflection, with some global considerations. Journal of Geophysical Research 101, 16259–16271.

Stammer, D., Wunsch, C., 1999. Temporal changes in eddy energy of the oceans. Deep-Sea Research II 46, 77–108.

Strub, P.T., Chereskin, T.K., Niiler, P.P., James, C., Levine, M.D., 1997. Altimeter-derived variability of surface velocities in the California Current system 1. Evaluation of TOPEX altimeter velocity resolution. Journal of Geophysical Research 102, 12727–12748.

Wunsch, C., 1997. The vertical partition of oceanic horizontal kinetic energy. Journal of Physical Oceanography 27, 1770–1794.

Yu, Y., Emery, W.J., Leben, R.E., 1995. Satellite altimeter derived geostrophic currents in the western tropical Pacific during 1992–1993 and their validation with drifting buoy trajectories. Journal of Geophysical Research 100, 25069–25085.

Zlotnicki, V., Siedler, G., Klein, B., 1993. Can the weak surface currents of the Cape Verde Frontal Zone be measured with Altimetry? Journal of Geophysical Research 98, 2485–2493.